Supplement of Atmos. Chem. Phys., 22, 8787–8803, 2022
https://doi.org/10.5194/acp-22-8787-2022-supplement

Atmospheric Chemistry and Physics
Open Access

Supplement of

Evolution of turbulent kinetic energy during the entire sandstorm process

Hongyou Liu et al.

Correspondence to: Xiaojing Zheng (xjzheng@lzu.edu.cn)

The validation of adaptive segmented stationary method

To validate the reliability of this method, a synthetic signal (as shown in Fig. S1a) is analyzed by using the adaptive segmented stationary method. The synthetic fluctuating signal consists of 7 components. Components 1–4 are amplitude variation signals with frequencies of 10 Hz, 5 Hz, 0.5 Hz and 0.1 Hz, respectively. Component 5 is an oscillation attenuation signal with a frequency of 1 Hz, Component 6 is a time-varying average, and component 7 is a real turbulent fluctuating signal provided in Wang and Zheng (2016). To enhance the non-stationarity of the synthetic signal, the amplitude of components 1-5 is increased monotonously with time. The IST of the signal is 79% (still 49% after removing the time-varying mean extracted by the EMD), indicating that the signal is non-stationary and cannot be directly analyzed by traditional statistical analysis methods. Therefore, the signal is segmented by employing the adaptive segmented stationary method, as shown in Fig. S1(b). The non-stationary signal is divided into three segments, and then the time-varying characteristics of the signal can be obtained by analyzing these three segments. Fig. S1 (c, d) shows the power spectra density and pre-multiplied spectra of these quasi-stationary signals and compared with the entire (unsegmented) turbulence fluctuating signal spectrum. It is seen in Fig. S1 (c) and S1 (d) that both the power spectra and the pre-multiplied spectra of the synthetic signal agree well with the spectrum of the turbulent fluctuating signal, except for a few extra peaks caused by the additional sinusoidal fluctuating signals. In addition, the energy at 1 Hz in the second and third segments decreases significantly because the amplitude of the oscillation attenuation component decreases with time. This indicates that the adaptive segmented stationary method can accurately exhibit the various frequency components contained in the signal and the time-varying characteristics when processing non-stationary signals. Therefore, the adaptive segmented stationary method is reliable to deal with non-stationary signals, and thus can be used to process the sandstorms data.

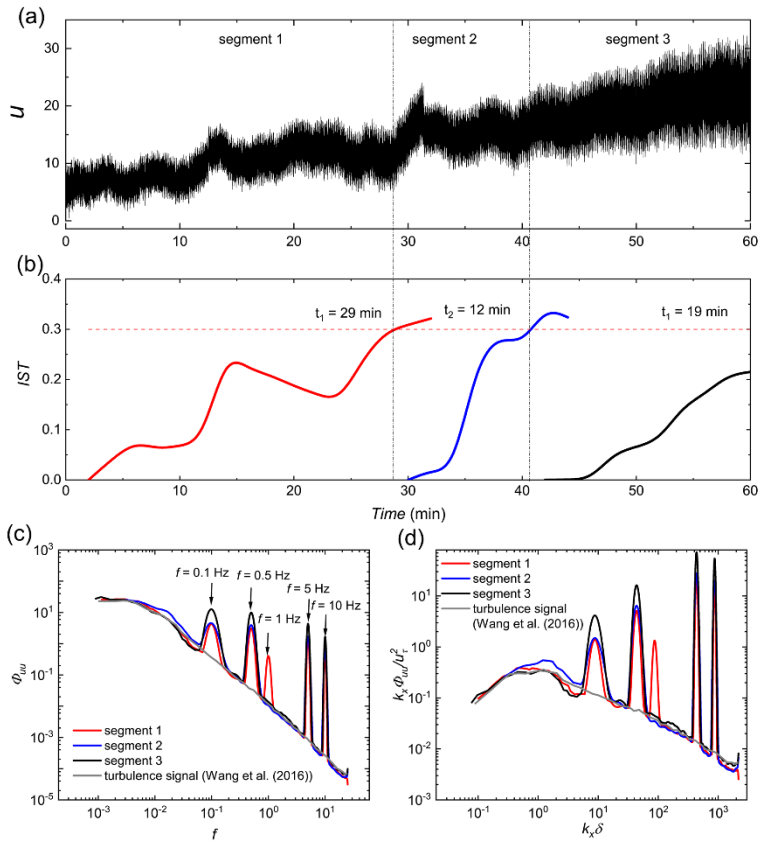

Figure S1. (a) Synthetic signal; (b) the change of the IST of the signal with time; (c) the power spectra density and (d) the pre-multiplied spectra of the synthetic signal. The gray line is the result of the entire (unsegmented) turbulent fluctuating signal contained in the synthetic signal. The red, blue and black lines represent the first, second and third segments of the signal, respectively.

Spectral method

The spectral method is a useful and important tool in data analysis. For a signal $x(t)$, the k th-order spectrum (or k -1 spectrum) can be obtained by a (k -1)-dimensional Fourier transform of the k th-order cumulant, which is given as

$$B_{k,x}(f_1, f_2, \cdots, f_{k-1}) = \sum_{m_1=-\infty}^{\infty} \cdots \sum_{m_{k-1}=-\infty}^{\infty} c_{k,x}(\tau_1, \tau_2, \cdots, \tau_{k-1}) exp\left[-j\sum_{i=1}^{k-1} f_i \tau_i\right] \quad \text{(S1)}$$

where $c_{kx}(\tau_1,\tau_2,\ldots,\tau_{k-1})$ is the k th-order cumulant of $x(t)$, τ_i (i=1,2,…,k-1) represents the temporal lead/lag, f_i is the frequency. In particular, when k=2, Equation (S1) represents the power spectrum,

$$P_{2,x}(f)=\sum_{m_1=-\infty}^{\infty} c_{2,x}(\tau)exp[-jf\tau]=\langle X(f)X^*(f)\rangle \tag{S2}$$

where <•> represents the expected value, $X(f)$ is the Fourier transform of a segment of the time series record, and the asterisk denotes the complex conjugate. The power spectrum represents the energy distribution at different frequencies. For studies on turbulence, the frequency is usually converts to the length scale by using Taylor's hypothesis of frozen turbulence, that is, $\lambda=\bar{u}/f$, where $\bar{u}$ is the velocity taken as the local mean. In addition, the pre-multiplied spectrum is obtained by multiplying the power spectral density by the frequency (or wavenumber).

When k=3 in Equation (S1), we can obtain the bispectrum,

$$\begin{aligned} B_{3,x}(f_1,f_2)&=\sum_{m_1=-\infty}^{\infty}\cdots\sum_{m_2=-\infty}^{\infty} c_{3,x}(\tau_1,\tau_2)exp\left[-j\left(f_1\tau_1+f_2\tau_2\right)\right] \\ &=\langle X(f_1)X(f_2)X^*(f_1+f_2)\rangle \end{aligned} \tag{S3}$$

which provides a measure of the quadratic interaction exhibited by the given triad of waves at frequencies of f_1, f_2 and f_3 that satisfy the resonance wave matching requirement $f_3 = f_1 + f_2$ (Hajj et al., 1997; Liu et al., 2019). And a nonzero bispectrum value means that phase coupling may occur between f_1, f_2 and f_3. As example, Fig. S2 shows the absolute bispectrum of the high frequency band of the streamwise velocity fluctuations in the sandstorm, where Fig. S2 (a) is the three-dimensional perspective and Fig. S2 (b) is the color contour map. It is seen that the bispectrum exists multiple peaks at different positions, indicating a strong quadratic phase coupling between the corresponding frequencies. In addition, the unphysical negative frequencies are derived from the process of bispectrum calculation. Thus, only the positive frequency component, that is, the first quadrant part, will be shown in the following study.

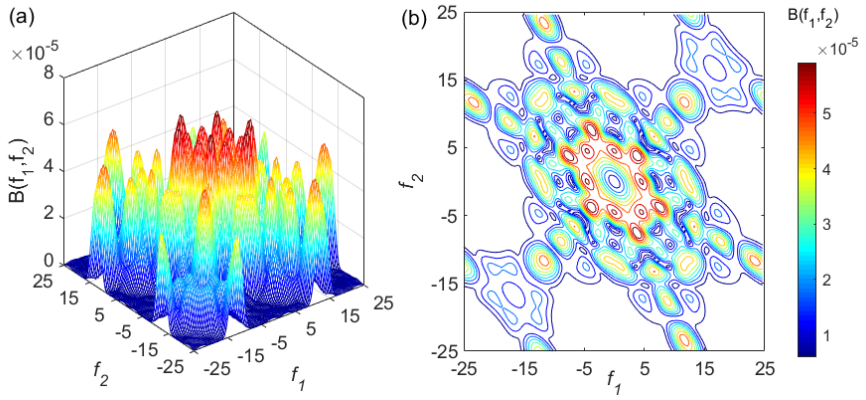

Figure S2. Bispectrum of the high frequency band of the streamwise velocity fluctuations in the sandstorm, (a) three-dimensional view, (b) colour contour map

To estimate the energy transfer process, the turbulent system can be represented by a nonlinear model, which are describable by a set of source ("input") signals X and the response ("output") signals Y. The model consists of linear, quadratic and higher order nonlinear elements (Ritz and Powers, 1986; Ritz et al., 1989),

$$Y_f = L_f X_f + \sum Q_f^{f_1,f_2} X_{f_1} X_{f_2} + \sum Q_f^{f_1,f_2,f_3} X_{f_1} X_{f_2} X_{f_3} + \cdots + \varepsilon_f \tag{S4}$$

where, $L_f X_f$ represents the linear transfer $Q_f^{f_1,f_2} X_{f_1} X_{f_2}$, represents the three wave process, $Q_f^{f_1,f_2,f_3} X_{f_1} X_{f_2} X_{f_3}$ represents the four wave process and ε_f is error term. Generally, the four wave process and the higher-order processes are much weaker than the three wave process (Ritz and Powers, 1986; Ritz et al., 1989), and thus Equation (S4) is simplified as

$$Y_f = L_f X_f + \sum_{\substack{f_1 > f_2 \\ f = f_1 + f_2}} Q_f^{f_1,f_2} X_{f_1} X_{f_2} + \varepsilon_f \tag{S5}$$

By multiplying Eq. (S5) with the complex conjugate of the input signal X_f, neglecting the error term and expressing the process in terms of time derivatives, we can obtain the wave kinetic equation (Ritz et al., 1989; Cziegler et al., 2013):

$$\frac{\partial P_f}{\partial t} = \gamma_f P_f + \sum_{f_1, f_2} T_f(f_1, f_2) \tag{S6}$$

where $P_f = < Y_f X_f^* >$ is the power spectrum, $\frac{\partial P_f}{\partial t}$ is the time change of the spectrum of frequency f, γ_f is the growth rate at the frequency f; $Q_f^{f_1,f_2}$ is the nonlinear transfer function, and $T_f(f_1, f_2) = |Q_f^{f_1,f_2}| < X_{f_1} X_{f_2} X_f^* >= |Q_f^{f_1,f_2}| B(f_1, f_2)$ is the nonlinear energy transfer function of the system, which represents a net flow of energy into or away from a given frequency f. Since we are concentrating on the effects of the nonlinear energy transfer in the process of sandstorm, the nonlinear transfer term under more scrutiny is $T_f(f_1,f_2)$. Eq.(S6) makes it clear that if $T_f(f_1,f_2)$ is positive (negative), the components at "target" frequency f_2 are gaining (losing) power and the components at the "source" frequency f_1 are losing (gaining) it via the convection represented in the X_{f2} term(Ritz et al., 1989; Cziegler et al., 2013).

For a turbulent system, where many waves interact with one frequency, the contribution of any given three components will be weaken, but the sum of all possible three components interactions can result in a significant change of power at this frequency (Ritz et al., 1989). Thus, by integrating the bispectrum along one of the frequency directions, we can obtain the integral bispectrum, which is defined as

$$AIB(f_1) = \int B(f_1, f_2) df_2 \tag{S7}$$

where $B(f_1,f_2)$ is the bispectrum of the signal. The integral bispectrum represents the total nonlinear interactions by all of the other frequency components on a certain frequency. It should be emphasized that f_1 and f_2 have the same meaning in the auto-bispectrum. Eq. (S6) and (S7) infer that when the integral bispectrum is positive (negative), the components at frequency f_2 are gaining (losing) power from the interaction with all of the possible components.

References

Cziegler, I., Diamond, P. H., Fedorczak, N., Manz, P., Tynan, G. R., Xu, M., Churchill, R. M., Hubbard, A. E., Lipschultz, B., Sierchio, J. M., Terry, J. L., and Theiler, C.: Fluctuating zonal flows in the I-mode regime in Alcator C-Mod, Phys Plasmas, 20, https://doi.org/10.1063/1.4803914, 2013

Hajj, M. R., Miksad, R. W., and Powers, E. J.: Perspective: Measurements and analyses of nonlinear wave interactions with higher-order spectral moments, J Fluid Eng-T Asme, 119, 3–13, https://doi.org/10.1115/1.2819116, 1997.

Liu, X. L., Yi, S. H., Xu, X. W., Shi, Y., Ouyang, T. C., and Xiong, H. X.: Experimental study of second-mode wave on a flared cone at Mach 6, Phys. Fluids, 31, https://doi.org/10.1063/1.5103192, 2019.

Ritz, C. P. and Powers, E. J.: Estimation of Nonlinear Transfer-Functions for Fully-Developed Turbulence, Physica D, 20, 320–334, https://doi.org/Doi 10.1016/0167-2789(86)90036-9, 1986.

Ritz, C. P., Powers, E. J., and Bengtson, R. D.: Experimental measurement of three-wave coupling and energy cascading, Phys. Fluids B-Plasma Physics, 1, 153–163, https://doi.org/10.1063/1.859082, 1989.

Wang, G. H. and Zheng, X. J.: Very large scale motions in the atmospheric surface layer: a field investigation, J. Fluid Mech., 802, 464–489, https://doi.org /10.1017/jfm.2016.439, 2016.